

Photoinduced η -pairing in One-dimensional Mott Insulators

Satoshi EJIMA^{1,2}, Tatsuya KANEKO³, Florian LANGE¹, Seiji YUNOKI^{2,4,5},
Holger FEHSKE¹

¹ *Institut für Physik, Universität Greifswald, D-17489 Greifswald, Germany*

² *Computational Condensed Matter Physics Laboratory, RIKEN Cluster for Pioneering Research (CPR), Wako, Saitama 351-0198, Japan*

³ *Department of Physics, Columbia University, New York, NY 10027, USA*

⁴ *Computational Quantum Matter Research Team, RIKEN Center for Emergent Matter Science (CEMS), Wako, Saitama 351-0198, Japan*

⁵ *Computational Materials Science Research Team, RIKEN Center for Computational Science (R-CCS), Kobe, Hyogo 650-0047, Japan*

E-mail: ejima@physik.uni-greifswald.de

(Received September 15, 2019)

Employing the density-matrix renormalization group technique in the matrix-product-state representation, we investigate the photoexcited superconducting correlations induced by the η -pairing mechanism in the half-filled Hubbard chain. We estimate the characteristic pair correlation function and verify the accuracy of our numerical results by comparison with exact-diagonalization data for small systems. The optimal parameter set of the pump that most enhances the η -pair correlations, is calculated in the strong-coupling regime. For such a pump, we explore the possibility of quasi-long-range order.

KEYWORDS: superconducting correlations, Hubbard model, DMRG

1. Introduction

Superconductivity is one of the most fascinating phenomena in condensed-matter physics and has attracted continuous attention since its discovery in 1911 [1, 2]. While the basic features of the superconducting (SC) phase are well established for equilibrium systems, the photoinduced superconductivity is subject of intense research because of the recent pump-probe experiments, e.g., in copper oxides [3–5] or in K_3C_{60} [6]. In these materials, the transient optical spectra imply the SC-like properties even at elevated temperatures.

Very recently, it was theoretically demonstrated that unconventional SC correlations can be induced by pulse irradiation in a simple Mott insulator described by the half-filled Hubbard model [7]. This SC state stems from the so-called η -pairing mechanism [8–10], characterized by staggered pair-density-wave oscillations in the off-diagonal long-range correlations [11]. However, since these results were obtained by the exact diagonalization (ED) technique, the accessible system size was only $L \lesssim 16$ with periodic boundary conditions (PBC) [7]. It is, thus, vitally important to discuss the finite-size effects in the η -pairing state and pair correlations especially at larger distances.

To make progress in this direction, we focus on one-dimensional systems, where the unbiased density-matrix renormalization group (DMRG) technique [13] can be applied. (We note that η -pairing state in the photoexcited state can also be found in two dimensions [7], but is hard to calculate in an approximation-free way). Simulating the real-space pair correlation

function and its structure factor, we explore the conditions under which η -pairing is most likely. For large enough system sizes, we demonstrate a peculiar increase of the pair structure factor with the parameter set of maximally enhanced η -pairing state after the photo excitation, which might be the signature of the (quasi-)long-range order of pairs.

2. Theoretical approach

Model. Hereinafter, we study the photoinduced η -pairing state in a half-filled Hubbard chain, defined by

$$\hat{H} = -t_h \sum_{j,\sigma} \left(\hat{c}_{j,\sigma}^\dagger \hat{c}_{j+1,\sigma} + \text{h.c.} \right) + U \sum_j \hat{n}_{j,\uparrow} \hat{n}_{j,\downarrow}, \quad (1)$$

where $\hat{c}_{j,\sigma}^\dagger$ ($\hat{c}_{j,\sigma}$) creates (annihilates) an electron with spin projection $\sigma = \uparrow, \downarrow$ at Wannier site j , and $\hat{n}_{j,\sigma} = \hat{c}_{j,\sigma}^\dagger \hat{c}_{j,\sigma}$. The transfer amplitude t_h enables the electrons to hop between neighboring lattice sites, whereas the on-site Coulomb repulsion U tends to localize the electrons, establishing a Mott insulating ground state.

Introducing a time-dependent external field into the hopping term by the Peierls substitution [14], $t_h \hat{c}_{j,\sigma}^\dagger \hat{c}_{j+1,\sigma} \rightarrow t_h e^{iA(t)} \hat{c}_{j,\sigma}^\dagger \hat{c}_{j+1,\sigma}$, where $A(t)$ is the time-dependent vector potential

$$A(t) = A_0 e^{-(t-t_0)^2/(2\sigma_p^2)} \cos[\omega_p(t-t_0)] \quad (2)$$

with amplitude A_0 , frequency ω_p and pulse width σ_p centered at time t_0 (> 0), makes the Hamiltonian time-dependent: $\hat{H} \rightarrow \hat{H}(t)$. As a consequence the equilibrium ground state $|\psi(0)\rangle$ at $t = 0$ evolves in time $|\psi(t)\rangle$. To take account of this time evolution, in our numerics, we apply the time-evolving block decimation method [15] in combination with the second-order Suzuki–Trotter decomposition. In the following, we use t_h (t_h^{-1}) as the unit of energy (time), and the time step δt is set to be $\delta t \cdot t_h = 0.01$.

Pairing correlations. The photoinduced η -pairing state can be characterized by the real-space pair correlation function

$$P(r, t) = \frac{1}{N_b} \sum_{j=1}^{N_b} \langle \psi(t) | \left(\hat{\Delta}_{j+r}^\dagger \hat{\Delta}_j + \text{h.c.} \right) | \psi(t) \rangle \quad (3)$$

with the on-site singlet pair operator $\hat{\Delta}_j = \hat{c}_{j,\uparrow} \hat{c}_{j,\downarrow}$. Here, $N_b = L - r$ denotes the number of pairs of sites separated by distance r in a system of L sites with open boundary conditions (OBC). For $r = 0$ the pair correlation is equal to twice the double occupancy, i.e., $P(r = 0, t) = 2n_d(t)$, where $n_d(t) = (1/L) \sum_{j=1}^L \langle \psi(t) | \hat{n}_{j,\uparrow} \hat{n}_{j,\downarrow} | \psi(t) \rangle$ as demonstrated in Ref. [7]. Note that it is important to analyze the Fourier transform of $P(r, t)$, i.e., $P(q, t) = \sum_r e^{iqr} P(r, t)$, which shows a characteristic enhancement after the pulse irradiation in the half-filled Hubbard model.

Accuracy check. Before we show our main results, we like to discuss the accuracy of the time-dependent DMRG simulations with OBC. During a DMRG simulation one chooses the maximum of the so-called bond dimension χ and makes sure that the truncation error in the singular value decomposition stays sufficiently small. The other way around, the maximum truncation error can also be fixed in the simulation. Figure 1 demonstrates the latter case, simulating the pair structure factor $P(q = \pi, t)$ by DMRG. The DMRG data are compared with ED results in Fig. 1(a) for $L = 12$. Keeping the cutoff smaller than 1×10^{-7} , $P(q = \pi, t)$ obtained by DMRG is in perfect agreement with the ED results, even up to time $t \cdot t_h = 80$.

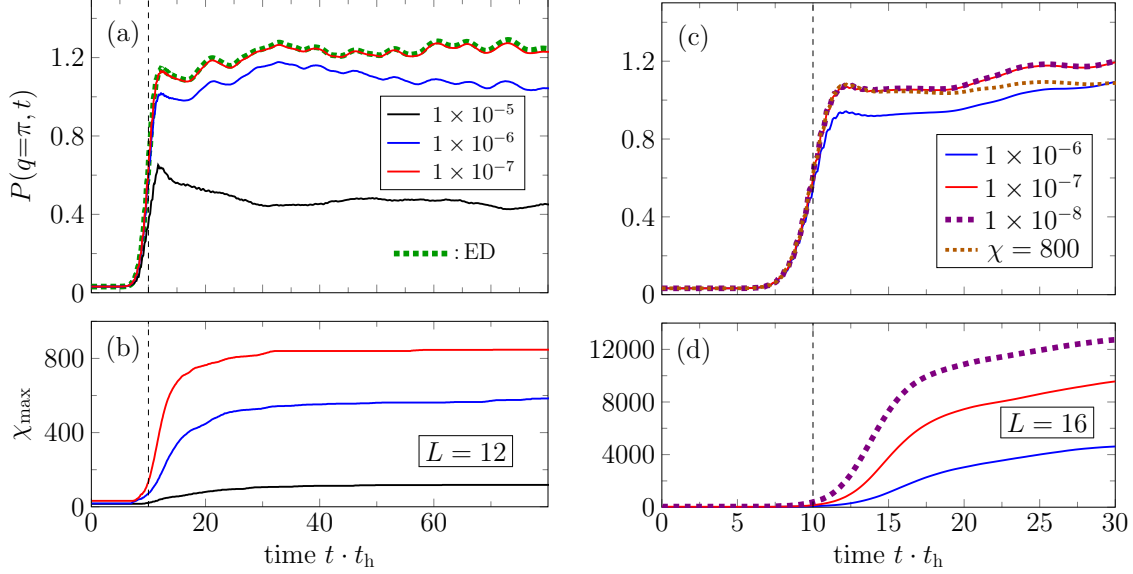


Fig. 1. Cutoff dependence of $P(q = \pi, t)$ for $U/t_h = 8$ within OBC DMRG (upper panels). Corresponding maximum bond dimension χ_{\max} needed to keep the maximum truncation error smaller than some fixed values at any time (lower panels). The dotted line in (a) is obtained by ED. $A(t)$ is parametrized by $A_0 = 0.4$, $\omega_p/t_h = 8$, $\sigma_p \cdot t_h = 2$ and $t_0 \cdot t_h = 10$.

The deviation only becomes significant when a larger cutoff is used for $t \gtrsim t_0$. In each case, the maximum bond dimension χ_{\max} increases rapidly around $t \sim t_0$ and afterwards stays constant for $t \cdot t_h \gtrsim 25$ [see Fig. 1(b)]. With increasing system size, the memory required by ED calculations increases exponentially: It is already problematic to carry out a time-dependent ED simulation for $L = 16$. Clearly the computational costs of the time-dependent DMRG calculations also increases with the system size L , but the truncation error can be kept below 1×10^{-8} in the case of $L = 16$. To keep the cutoff less than 1×10^{-7} up to $t \cdot t_h = 30$, χ_{\max} should be about 10000 as in Fig. 1(d). As shown by Fig. 1(c), the difference between the DMRG results for the maximum truncation errors 1×10^{-7} and 1×10^{-8} is negligible. Thus, it is sufficient to keep the truncation error less than 1×10^{-7} in the time-dependent DMRG simulations. This is computationally expensive, however, due to the rapidly increasing bond dimensions. Alternatively, by keeping bond dimensions $\chi = 800$, reasonable agreement can also be obtained up to $t \cdot t_h \simeq 20$ [see the dotted line in Fig. 1(c)].

3. DMRG results

We now determine the optimal parameter set for the enhancement of $P(q = \pi, t)$ and examine the behavior of the pair correlations for these parameters. Figure 2 gives the OBC DMRG contour plots of $P(\pi, t)$ at various times for different values of A_0 and ω_p . For $t < t_0$, the magnitude of the pair correlation functions is still marginal. When $t \gtrsim t_0$, a noticeable enhancement of pair correlations appears in wide parameter regions. Furthermore, the spectral intensity of $P(\pi, t)$ is concentrated in a single spot after pulse irradiation ($t \cdot t_h \gtrsim 20$). Interestingly, the height of the peak at $\omega_p/t_h \simeq 6.8$ and $A_0 \simeq 0.4$ increases at long times $t \cdot t_h = 30$. Figure 2 also demonstrates the system-size dependence of the pair structure factor. For $L = 8$ (upper panels of Fig. 2) the stripe structure can be observed after the pulse irradiation as in the case of ED results with $L = 14$ [7]. As explained in Ref. [7], the peak structure of $P(\pi, t)$ is essentially the same as the ground-state optical spectrum $\chi_{JJ}(\omega)$ with some Lorentzian

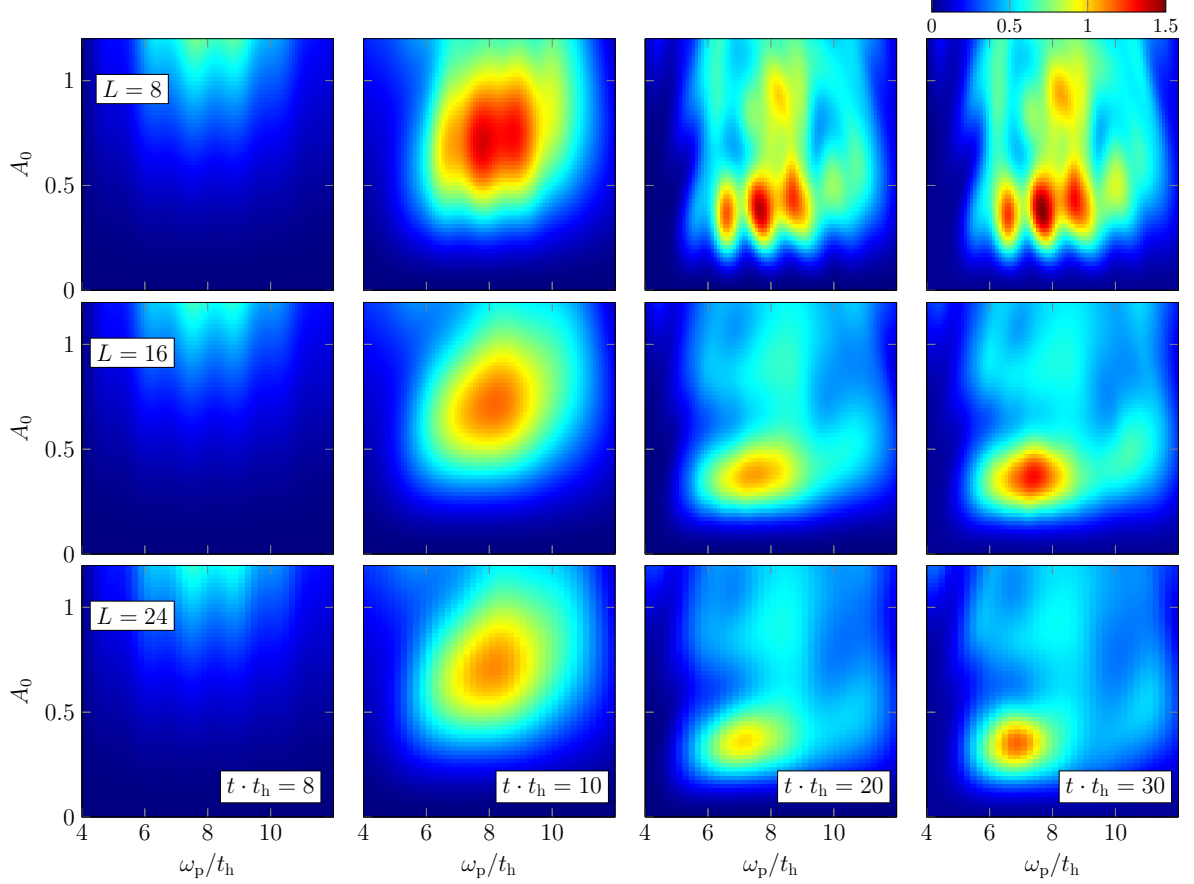


Fig. 2. Contour plot of $P(q = \pi, t)$ at $t \cdot t_h = 8, 10, 20$, and 30 for $U/t_h = 8$, $\sigma_p = 2$ and $t_0 \cdot t_h = 10$ in the ω_p - A_0 plane. All data obtained by DMRG with bond dimensions $\chi = 800$.

broadening η_L , depending on $1/\sigma_p$. If the system size is too small for some (small) η_L , the spectrum is described by a series of peaks. The stripe structure found in $P(\pi, t)$ for $L = 8$ reflects this finite-size effect. These stripes merge and construct a single peak structure for larger system sizes $L \geq 16$. With increasing L the enhanced regime is narrowed. Note that the value of $\omega_p \simeq 6.8$ at the peak position corresponds to about the size of the Mott gap Δ_c , i.e., the peak position of $\chi_{JJ}(\omega)$ can be estimated to be $\omega \sim 1.461\Delta_c \sim 6.84$ [16]. This is in accord with the DMRG data for $L = 24$, although Eq. (8) of Ref. [16] is only valid in the weak-coupling regime.

Let us analyze the pair correlations at the peak position of the contour plot for $L = 24$ and $t \cdot t_h = 30$, i.e., $A_0 = 0.36$ and $\omega_p/t_h = 6.8$. Obviously, after the pulse irradiation, $P(\pi, t)$ keeps increasing gradually for $t \cdot t_h \gtrsim 20$, as shown in Fig. 3(a), while $P(\pi, t)$ by ED with PBC saturates at some constant value [7]. Note that the results do not depend strongly on bond dimensions for large times. Figure 3(b) displays the real-space pair correlation function. $P(r, t)$ for $t \cdot t_h = 30$ is clearly enhanced for large distances $r \gtrsim L/2$ comparing with those for $t \cdot t_h = 20$.

Of course, $L = 24$ is still too small to examine the behavior of correlation functions and boundary effects are showing up in $P(r, t)$ for large distances. Moreover, the definition of the pair correlation with OBC, Eq. (3), is not equivalent to the usual ones with PBC in Ref. [7]. These data, however, might imply the possibility of a (quasi-)long-range order of η -pairs, i.e.,

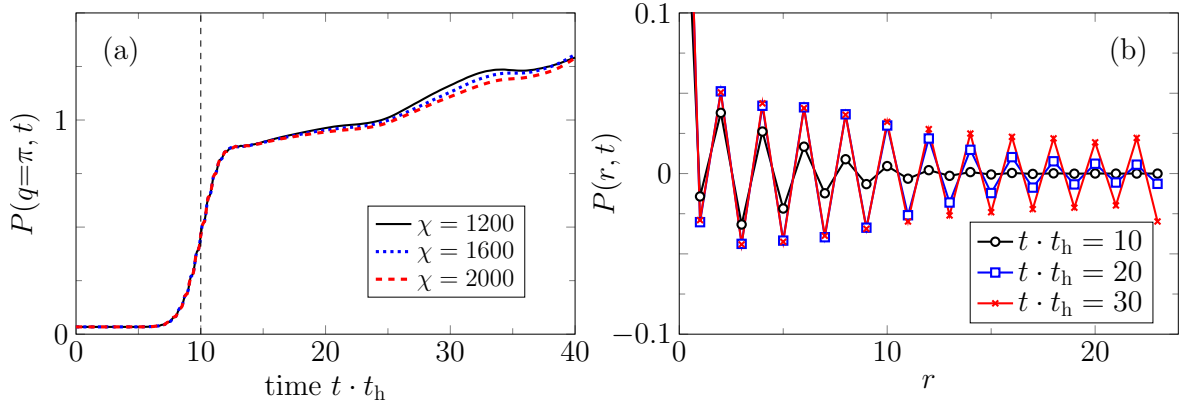


Fig. 3. Time evolution of $P(q = \pi, t)$ [panel (a)] and $P(r, t)$ [panel (b)] for $U/t_h = 8$, $\sigma_p = 2$ and $t_0 \cdot t_h = 10$, where $L = 24$ with OBC. Parameters of the pump are $A_0 = 0.36$ and $\omega_p/t_h = 6.8$, which corresponds to a maximum of $P(\pi, t)$ at $t \cdot t_h = 30$ in Fig. 2.

the power-law decay of pair correlations for large times. Further studies for larger system sizes are desirable.

4. Summary

In conclusion, we demonstrated η -pairing in the one-dimensional Hubbard model at half filling by means of unbiased density-matrix renormalization group simulations. For small system sizes, the time evolution of the corresponding pair correlation functions can be computed with high accuracy—i.e., the maximum truncation error is always less than 1×10^{-8} —up to times $t \cdot t_h = 80$ (30) for $L = 12$ (16) with open boundary conditions. Although the numerical accuracy will get worse as L increases, the resonant parameter set can be determined up to $L = 24$. For these pump parameters the pair structure factor $P(q = \pi, t)$ is enhanced and magnitude of the pair correlation functions increases for long distances with time after pulse irradiation. This can be taken as strong indication for η -pairing and off-diagonal (quasi) long-range order. Since boundary effects still show up in the pair correlation simulation data, it is highly desirable to prove quasi-long-range order for larger system sizes or, even better, directly in the thermodynamic limit by using, e.g., the infinite time-evolving block decimation approach [17].

Acknowledgments

We thank S. Miyakoshi and T. Shirakawa for useful discussions. T.K. was supported by the JSPS Overseas Research Fellowship, F.L. by Deutsche Forschungsgemeinschaft (Germany) through Project No. FE 398/8-1, and S.Y. by Grants-in-Aid for Scientific Research from JSPS (Project No.: JP18H01183) of Japan. The DMRG simulations were performed using the ITensor library [18].

References

- [1] E. Dagotto, Rev. Mod. Phys. **66**, 763 (1994).
- [2] P. A. Lee, N. Nagaosa, and X.-G. Wen, Rev. Mod. Phys. **78**, 17 (2006).
- [3] D. Fausti, R. I. Tobey, N. Dean, S. Kaiser, A. Dienst, M. C. Hoffmann, S. Pyon, T. Takayama, H. Takagi, and A. Cavalleri, Science **331**, 189 (2011).

- [4] W. Hu, S. Kaiser, D. Nicoletti, C. R. Hunt, I. Gierz, M. C. Hoffmann, M. L. Tacon, T. Loew, B. Keimer, and A. Cavalleri, *Nat. Mater.* **13**, 705 (2014).
- [5] R. Mankowsky, A. Subedi, M. Först, S. O. Mariager, M. Chollet, H. T. Lemke, J. S. Robinson, J. M. Glownia, M. P. Minitti, A. Frano, M. Fechner, N. A. Spaldin, T. Loew, B. Keimer, A. Georges, and A. Cavalleri, *Nature* **516**, 71 (2014).
- [6] M. Mitrano, A. Cantaluppi, D. Nicoletti, S. Kaiser, A. Perucchi, S. Lupi, P. Di Pietro, D. Pontiroli, M. Riccò, S. R. Clark, D. Jaksch, and A. Cavalleri, *Nature* **530**, 461 (2016).
- [7] T. Kaneko, T. Shirakawa, S. Sorella, and S. Yunoki, *Phys. Rev. Lett.* **122**, 077002 (2019).
- [8] C. N. Yang, *Phys. Rev. Lett.* **63**, 2144 (1989).
- [9] F. H. L. Essler, V. E. Korepin, and K. Schoutens, *Phys. Rev. Lett.* **67**, 3848 (1991).
- [10] F. H. L. Essler, V. E. Korepin, and K. Schoutens, *Nucl. Phys. B* **372**, 559 (1992).
- [11] See also Ref. [12] for analogous electron-electron pair correlations of spinless fermions induced by the pulse irradiation in the excitonic insulator.
- [12] R. Fujiuchi, T. Kaneko, Y. Ohta, and S. Yunoki, *Phys. Rev. B* **100**, 045121 (2019).
- [13] S. R. White, *Phys. Rev. Lett.* **69**, 2863 (1992).
- [14] R. Peierls, *Z. Phys.* **80**, 763 (1933).
- [15] G. Vidal, *Phys. Rev. Lett.* **91**, 147902 (2003).
- [16] E. Jeckelmann, F. Gebhard, and F. H. L. Essler, *Phys. Rev. Lett.* **85**, 3910 (2000).
- [17] G. Vidal, *Phys. Rev. Lett.* **98**, 070201 (2007).
- [18] <http://itensor.org/>.